Available online at www.sciencedirect.com
ScienceDirect
Journal of Environmental Sciences 21(2009) 520–526
JOURNAL OF ENVIRONMENTAL SCIENCES
ISSN 1001-0742
CN 11-2629/X
www.jesc.ac.cn

Relation of lead adsorption on birnessites with different average oxidation states of manganese and release of $Mn^{2+}/H^+/K^+$

ZHAO Wei, FENG Xionghan, TAN Wenfeng, LIU Fan, DING Shuwen*

Key Laboratory of Subtropical Agriculture Resource & Environment, Ministry of Agriculture of China, Huazhong Agricultural University, Wuhan 430070, China. E-mail: aoei@webmail.hzau.edu.cn

Received 13 May 2008; revised 02 August 2008; accepted 15 August 2008

Abstract

The characteristics of Pb^{2+} adsorption on the surface of birnessites with different average oxidation states (AOS) of Mn, synthesized under acidic and alkali conditions, were investigated. The results indicated that the amount of adsorbed Pb^{2+} increased with the increase of Mn AOS in birnessites. The amount of Pb^{2+} adsorbed positively correlated with the amount of released Mn^{2+}, H^+, and K^+ (r = 0.9962 > 0.6614, n = 14, α = 0.01). The released Mn^{2+}, H^+, and K^+ were derived mostly from the corresponding cations adsorbed on the vacant sites. The maximum amount of adsorbed Pb^{2+} increased with the increasing vacant cation sites, leading to an increase of the total amount of released Mn^{2+}, H^+, and K^+, and the increased likelihood for two Pb^{2+} adsorbed in the region of one side of a vacant site.

Key words: Pb^{2+}; adsorption; birnessite; vacant site; cation release

DOI: 10.1016/S1001-0742(08)62302-5

Introduction

Hydrogen ion (H^+) released during adsorption process of heavy metals onto iron, aluminum, and manganese oxides due to the complexation reactions between heavy metals and hydroxyl group located on the oxides. Many researchers attempted to understand adsorption forms of (M^{2+}) on the oxide surface using the ratio of released H^+ to adsorbed M^{2+} (Mckenzie, 1979, 1980a, 1980b; Murray, 1975). When the ratio of H^+/M^{2+} equals 0, 1, or 2, the corresponding adsorption forms of M^{2+} were M^{2+}, MOH^+, or $M(OH)_2$, respectively (Anderson and Christensen, 1988; Spark *et al.*, 1995). However, because of the difference among the hydrolysis characteristics of different heavy metals, H^+/M^{2+} varied from 1 to 2. For example, for the Pb^{2+}, Cd^{2+}, Zn^{2+} adsorption onto the hydrous manganese oxide, the ratio of H^+/M^{2+} was 1.4, 1.3 and 1.1, respectively (Gadde and Laitinen, 1974). Some researchers concluded that H^+/M^{2+} of Pb^{2+} adsorption on γ-Al_2O_3 is 1.5, and Pb^{2+} formed an inner-sphere, monodentate complex with oxygen atoms on the surface through Reactions (1) and (2) (Hohl and Stumm, 1976) or Reaction (3) (Davis and Leckie, 1978):

$$AlOH_{surface} + Pb^{2+}(aq) \rightleftharpoons AlO_{surface}\text{-}Pb^+ + H^+ \quad (1)$$

$$2AlOH_{surface} + Pb^{2+}(aq) \rightleftharpoons (AlO_{surface})_2\text{-}Pb + 2H^+ \quad (2)$$

$$AlOH_{surface} + Pb^{2+}(aq) + H_2O \rightleftharpoons AlO^-_{surface} - Pb(OH)^+ + 2H^+ \quad (3)$$

Therefore, only based on the ratio of H^+ released to M^{2+} adsorbed, it was difficult to determine adsorption form of a heavy metal on the surface of oxides. Besides H^+, other released cations such as Mn^{2+} and K^+ could be considered to affect the behavior of Pb adsorption. There should be an intrinsic relation between the amount of the released cation and the amount of a heavy metal adsorbed. Clearly, the analysis for the total amounts of individual cation released will help us to understand the adsorption form of heavy metals on oxides.

Lead is a heavy metal of particular concern in the environment, and its fate has always attracted extensive attention. Manganese oxides are extensively distributed in soils, sediments and ocean manganese nodules (O'Reilly and Hochella, 2003). They commonly have a lower point of zero charge, large specific surface area and great amounts of negative charge, and are highly active in various chemical reactions. They are considered as an important lead adsorbent (Mckenzie, 1980a; O'Reilly and Hochella, 2003; Post, 1999). The phyllomanganate birnessite is the most common among manganese oxides in soils, and Mn oxides can be synthesized by direct or indirect transformation of birnessite (Golden *et al.*, 1987; Tu *et al.*, 1994). MnO_6 layers of birnessite comprise edge-sharing Mn(IV)O_6 octahedra, Mn(III)O_6 octahedra and cation vacancies (Villalobos *et al.*, 2006). Some Mn^{3+} and Mn^{2+} are located above or below cation vacancies

* Corresponding author. E-mail: dingshuwen@mail.hzau.edu.cn

(Webb *et al*., 2005). Previous studies have indicated that the vacancies in the structure of birnessite commonly account for the negatively charged layer partially causing adsorption of Pb, Zn, Cu, Cd and Ni, oxidation of Co^{2+}, Cr^{3+} and conversion of minerals (Appelo and Postma, 1999; Burns, 1976; Lanson *et al*., 2002a; Manceau and Charlet, 1992; Peacock and Sherman, 2007; Villalobos *et al*., 2006). To some extent, the amount of vacant sites in birnessite increased with the increase of Mn AOS (Zhao *et al*., 2009). Therefore, through the experiments of the Pb^{2+} adsorption onto birnessite with different Mn AOS, the relation between the total amount of released cation and the amount of adsorbed heavy metal was elucidated. Along with the structural characteristics of birnessite, the relation between the origin of released cation and structure of birnessite was investigated to further understand adsorption mechanism of Pb^{2+} onto birnessite.

1 Materials and methods

1.1 Synthesis of birnessite

In acidic media, birnessite was synthesized according to the method of McKenzie (1971). Synthetic birnessites designated HB1, HB2, HB3, HB4, HB5, and HB6, respectively, were prepared using 45, 53.3, 53.3, 45, and 66.7 mL of 6 mol/L HCl, and 55-mL of 8 mol/L HCl added dropwise at a speed of 0.7 mL/min to a 0.2-mol boiling $KMnO_4$ solution in 300–400 mL of distilled deionized water. The solution was stirred during the reaction. After further boiling for 30 min, the products were aged at 60°C for 12 h according to Feng *et al*. (2007).

In alkali media, birnessite was prepared by the method of Villalobos *et al*. (2003). A 125-mL solution of 0.364, 0.364, 0.444, 0.444, 0.444, 0.5, 0.6, 0.6 mol/L $MnCl_2$ was mixed, respectively, with 6.3 mol/L KOH in 125 mL of distilled deionized water to form a pink $Mn(OH)_2$ gel precipitate. A 250-mL of 0.1 mol/L $KMnO_4$ was added at a rate of 3 mL/min into the mixture solution and stirred to form a dark grey precipitate. The final molar ratio of Mn(VII)/Mn(II) in the reaction was 0.55, 0.55, 0.45, 0.45, 0.45, 0.4, 0.33 and 0.33, respectively. After stirring for 30 min, the products were aged at 60°C for 12 h. The samples obtained were named as OHB1, OHB2, OHB3, OHB4, OHB5, OHB6, OHB7 and OHB8. All samples were purified by electrical dialysis with a voltage range 150–220 V. When the conductivity of the supernatant was below 20 μS/cm, samples were dried at 40°C.

1.2 Characterization

X-ray diffraction (XRD) analysis was performed on a D/Max-3B diffractometer (Rigaku, Japan) with monochromated Fe K_α radiation. The diffractometer was operated at a tube voltage of 40 kV and a tube current of 20 mA. Intensities were measured at an interval of $2\theta = 0.02°$ using a 0.2-s counting time per step.

Transmission electron microscopy (TEM) analysis was carried out with Philips-CM 12 (Philips, the Netherlands) operated at 120 kV. The samples were crushed to powder, and then dispersed in absolute alcohol and sonicated prior to deposition on a holey carbon film. The high resolution TEM examination was performed for the sample suspension dried on a holely carbon grid with a JEOL JEM 2010 FEF electron microscope (JEOL, Japan) at 200 kV.

1.3 Average oxidation state of Mn

The average oxidation state (AOS) of Mn was measured by the oxalic acid-permanganate back-titration method (Kijima *et al*., 2001). First, for the determination of total Mn content, 0.1 g of sample was dissolved in 25 mL of hydrochloric acid hydroxylamine and diluted to 250 mL. A 1-mL of the diluted solution was then diluted to 100 mL. The content of Mn was measured using flame atomic absorption spectrometry (AAS240FS model, Varian, Australia). Second, 0.1 g of the sample was completely dissolved in 5 mL of 0.5 mol/L $H_2C_2O_4$ and 10 mL of 1 mol/L H_2SO_4 to reduce all highly charged manganese ions to Mn^{2+}. The excess $C_2O_4^{2-}$ was determined by back-titration at 75°C with a standardized $KMnO_4$ solution. The AOS of Mn was calculated according to both the titration result and the total amount of Mn determined by atomic absorption spectrometry.

1.4 Adsorption experiments

Considering that Pb^{2+} can form precipitate with CO_3^{2-} easily, we set the pH of reaction system as 5 (at $C_{Pb^{2+}} \leqslant 0.01$ mol/L, $C_{Pb^{2+}} \times C_{CO_3^{2-}} \leqslant 3.199 \times 10^{-14} < K_{sp} = 7.4 \times 10^{-14}$). First, 5 g/L sample suspensions at pH 5.00 and a series of Pb^{2+} solutions at different concentrations (0–15 mmol/L) at pH 5.00 (ionic strength $I = 0.15$ adjusted with $NaNO_3$) were prepared. The pH of the suspensions was maintained at 5.00 by adding 0.1 mol/L HNO_3 or 0.1 mol/L NaOH. Then, 5 mL of sample suspensions were mixed with 10 mL solutions of various Pb^{2+} concentrations in 50-mL polyethylene centrifuge tubes. A ratio of 1.67 g/L for solid to liquid was obtained, the concentrations of Pb^{2+} were in the range of 0 to 10 mmol/L and ionic strength was 0.1 during the reaction. The tubes were then capped and shaken for 24 h at 25 ± 1°C. The pH of the reaction system was maintained at 5.00 ± 0.05 by adding a standardized solution of NaOH and/or HNO_3 using pH-stat technique. Finally, the tubes were centrifuged at 22400 ×*g* for 10 min in a Beckman super-speed refrigerated centrifuge (J2-MC model, Beckman, America). The supernatants were collected and analyzed for Pb^{2+} and Mn^{2+} concentration with a Varian AAS240FS, and for K^+ concentraiton with a flame spectrophotometer (M410 model, Sherwood, England). The amount of Pb^{2+} adsorbed and the amounts of Mn^{2+} and K^+ released during the whole adsorption process were obtained by comparing with a control solution. The amount of released H^+ was determined by the addition of amount of standardized solution of HNO_3 and/or NaOH. All the measurements were repeated three times.

2 Results

2.1 Characterization of the synthesized sample

Figure 1 shows the powder XRD patterns of the

synthesized birnessites. They were single phased birnessite from the XRD analyses. HB series were indicated by four characteristic peaks at 0.721, 0.361, 0.246, and 0.142 nm, while OHB series was indicated by five characteristic peaks at 0.725, 0.361, 0.247, 0.233, and 0.1425 nm, respectively. The AOS of Mn for samples are listed in Table 1.

Although the AOS of Mn differed among the birnessites prepared by different methods, the birnessites had similar morphology and size (Fig. 2). This indicates that the AOS of Mn influence the short-ranged structure or substructure of birnessite rather than the long-ranged structure as shown by XRD and TEM. The HB-series consisted of clusters of 100 to 200 nm spheroidal aggregates, which is consistent with the balls of needles described by McKenzie (1971). The balls, observed from high magnitude TEM, were randomly stacked thin plate aggregates (Feng *et al*., 2007). The OHB consisted of thin plates with irregular shape along the direction of the (001) plane with a size range 100–250 nm (Feng *et al*., 2004).

Table 1 Average oxidation state (AOS) of Mn for samples on birnessite

H-birnessite	AOS	OH-birnessite	AOS
HB1	3.92	OHB1	3.89
HB2	3.91	OHB2	3.76
HB3	3.88	OHB3	3.63
HB4	3.84	OHB4	3.60
HB5	3.83	OHB5	3.60
HB6	3.67	OHB6	3.58
		OHB7	3.51
		OHB8	3.49

2.2 Isothermal adsorption of heavy metals by two series of birnessites

Adsorption isotherms (Fig. 3) for HB and OHB were similar in shape, which could be assigned to L type according to Giles *et al*. (1960). When the equilibrium concentration of Pb^{2+} was increased, the amount of Pb^{2+} adsorbed increased sharply at the first stage, then reached plateau slightly. All adsorption isotherms were fitted by the Langmuir non-linear model, according to Eq. (4). The parameters are listed in Table 2.

$$Y = A_{\max}KC/(1 + KC) \quad (4)$$

where, Y (mmol/kg) is the adsorbed amount per unit weight, $A_{\max}$ represents the maximum adsorbed amount, C is the equilibrium concentration of heavy metals and K is a constant related to adsorption energy as a function of adsorption enthalpy and temperature (Kinniburgh, 1986). The maximum amount of Pb^{2+} adsorbed increased from 1320 to 2457 mmol/kg as the AOS of Mn in HB increased from 3.67 to 3.92. Similarly, the maximum amount of Pb^{2+} adsorbed increased from 500 to 1814 mmol/kg as the AOS

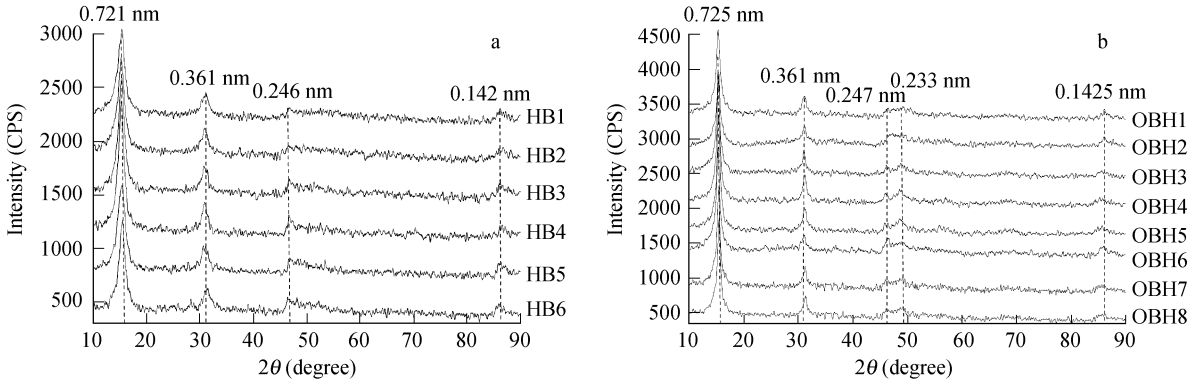

Fig. 1 XRD patterns of HB (a) and OHB (b) samples with different Mn average oxidation states (AOS).

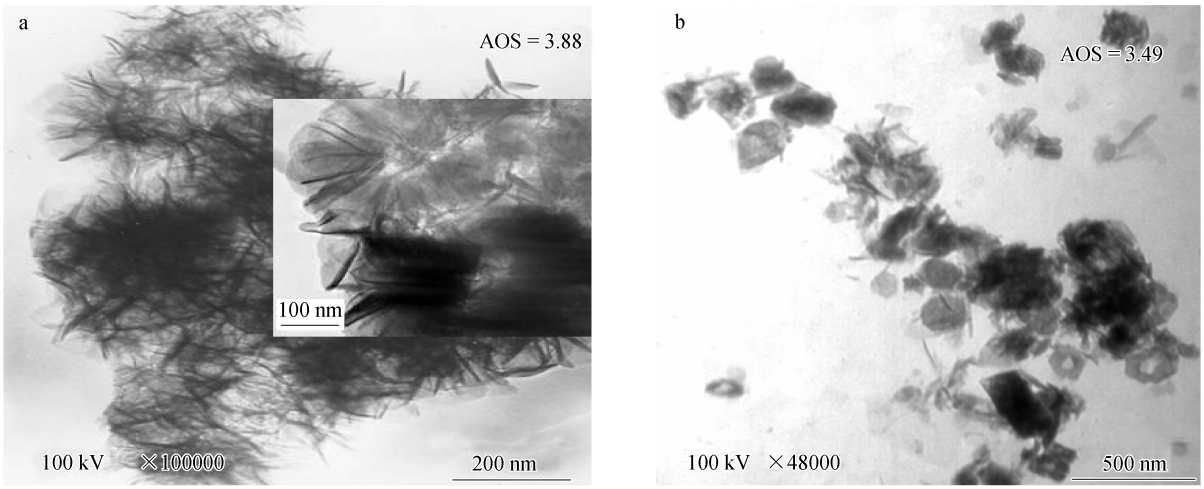

Fig. 2 TEM image of the synthesized birnessite HB3 (a) and OHB8 (b). TEM image of other samples was omitted.

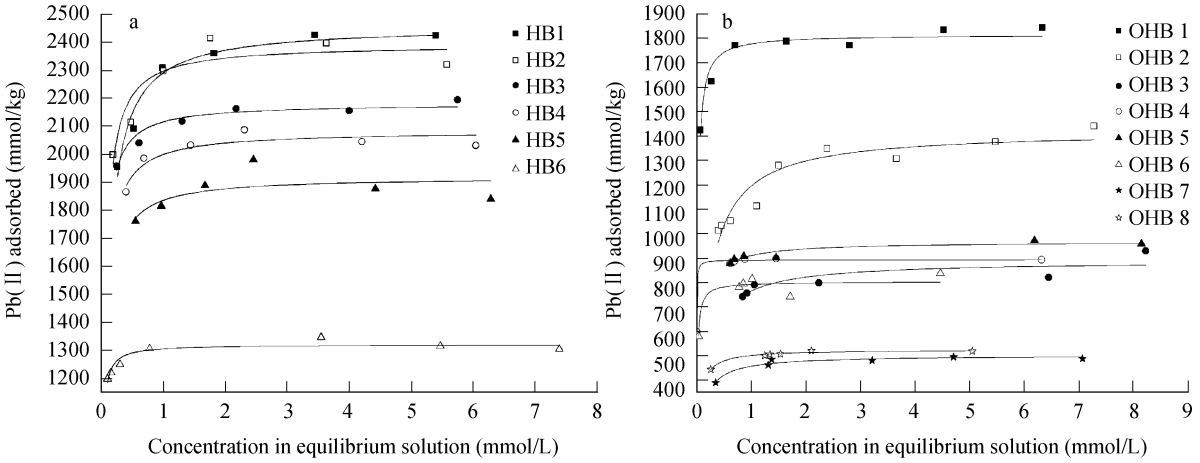

Fig. 3 Adsorption isotherms of Pb^{2+} on birnessite for HB (a) and OHB (b) at (25 ± 1)°C, pH 5.00, ionic strength 0.1 mol/L $NaNO_3$. The solution concentration of birnessite was 1.67 g/L.

Table 2 Langmuir parameters for adsorption of Pb^{2+}

Birnessite	A_{max} (mmol/kg)	K	r
H-birnessite			
HB1	2457	13.77	0.99
HB2	2391	24.33	0.99
HB3	2180	32.89	0.99
HB4	2082	24.15	0.99
HB5	1919	21.93	0.99
HB6	1320	86.96	0.99
OH-birnessite			
OHB1	1814	48.31	0.99
OHB2	1420	5.313	0.99
OHB3	887	6.238	0.99
OHB4	892	555.6	0.99
OHB5	966	16.13	0.99
OHB6	802	74.63	0.99
OHB7	500	10.31	0.99
OHB8	524	20.75	0.99

A_{max}: maximum adsorbed amount; K: constant related to adsorption energy.

Table 3 Maximum amount of released Mn^{2+}, H^+, K^+ during Pb^{2+} adsorption (mmol/kg)

Birnessite	Mn^{2+}	H^+	K^+	$H^+ + K^+$	$Mn^{2+} + H^+ + K^+$
HB1	0	2768	1195	3963	3963
HB2	0	2730	1103	3833	3833
HB3	0	2749	872	3621	3621
HB4	0	2514	811	3325	3325
HB5	0	2654	414	3068	3068
HB6	219	1735	273	2009	2228
OHB1	55	2527	525	3052	3107
OHB2	183	1720	317	2038	2220
OHB3	193	892	608	1500	1693
OHB4	218	980	375	1355	1573
OHB5	207	966	299	1265	1472
OHB6	216	1056	89	1177	1393
OHB7	143	573	160	733	876
OHB8	77	745	130	875	952

of Mn in OHB increased from 3.49 to 3.89 (Tables 1 and 2).

2.3 Release of Mn^{2+}, H^+, and K^+ during Pb adsorption

The maximum amounts of released Mn^{2+}, H^+, and K^+ during Pb adsorption varied with the changes in Mn AOS (Table 3). In the HB series, Mn AOS for HB1, HB2, HB3, HB4, and HB5 was high, and almost no Mn^{2+} was released. However, the Mn AOS for HB6 was the lowest among the HB samples with the maximum amount of released Mn^{2+} (219 mmol/kg). These results showed that the maximum amount of Mn^{2+} released decreased with the increase in Mn AOS, and the maximum amounts of released Mn^{2+} were similar for the samples with similar AOS value. For HB and OHB series, the maximum amount of released H^+ or K^+ tended to increase as the AOS of Mn increased (Tables 1 and 3).

3 Discussion

The amount of released Mn^{2+}, H^+, K^+ during Pb^{2+} adsorption positively correlated with the amount of Pb^{2+} adsorbed ($r = 0.9962 > 0.6614$, $n = 14$, $\alpha = 0.01$). Such a relationship reveals that the amount of Pb^{2+} adsorbed on birnessite was greatly related to the amount of vacant sites (Lanson *et al*., 2002b; Manceau *et al*., 2002). Therefore, Mn^{2+}, H^+, and K^+ released during the adsorption were derived mostly from the cations adsorbed onto the vacant sites (Gaillot *et al*., 2003; Lanson *et al*., 2000; Matocha *et al*., 2001).

It was reported that in the structure of birnessite, either a proton and a potassium ion (Gaillot *et al*., 2003; Villalobos *et al*., 2006), or two protons, Mn^{2+} or $(Mn(III)OH)^{2+}$ were located on each side of a vacant cation site to achieve local charge balance (Lanson *et al*., 2000). If only one Pb^{2+} was adsorbed on one side of a vacant site during the Pb adsorption, the following reactions could be applied to illustrate the process of the adsorption.

Process (1): a proton and a potassium are displaced from one side of a vacant site by Pb^{2+} adsorbed, the amount of adsorption sites occupied by Pb^{2+} equaled the amount of H^+ or K^+ released (Reaction (5)), with $V_1 = H_1 = P_1$ (subscript 1 stands for the first reaction, and the following subscripts stand for their respective reactions; V stands for the amount of adsorption sites, and H and P represent the amount of released H^+ and K^+ in the

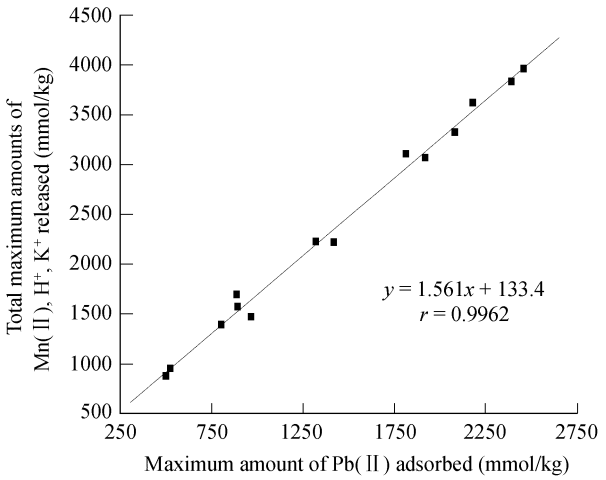

Fig. 4 Linear correlation between the total maximum amounts of released Mn^{2+}, H^+, K^+ and the maximum amount of Pb^{2+} adsorbed.

algebraic, respectively).

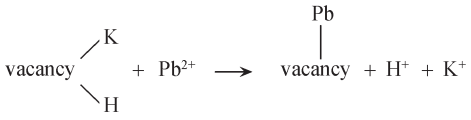

(5)

where, vacancy stands for one side of a vacant site.

Process (2): two protons are displaced from one side of a vacant site by Pb^{2+} adsorbed (Pb^{2+} adsorbed displaces two protons from particle edges of birnessite, and forms double-corner-sharing complex with oxygens on the surface, which can be equal to that case) (Reaction (6)), the relationship between the amount of adsorption sites occupied by Pb^{2+} and the amount of released H^+ was $V_2 = 1/2\ H_2$;

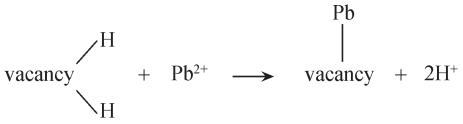

(6)

Process (3): one Mn^{2+} is displaced from one side of a vacant site by each Pb^{2+} being adsorbed (Reaction (7)), the relationship between the amount of adsorption sites occupied by Pb^{2+} and the amount of Mn^{2+} released was $V_3 = M_3$, M represent the amount of released Mn^{2+} in the algebraic;

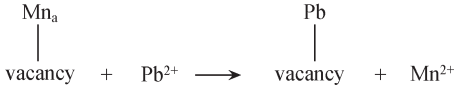

(7)

where, Mn_a stands for Mn^{2+} occupied on one side of a vacant site in the reaction equation.

Process (4): $(Mn(III)OH)^{2+}$ is displaced from one side of a vacant site by a Pb^{2+} being adsorbed (Recation (8)).

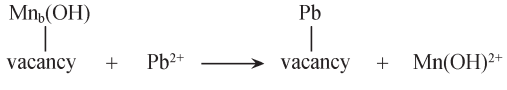

(8)

where, Mn_b stands for Mn(III) occupied on one side of a vacant site in the reaction equation, and taking into account the disproportion of Mn(III) displaced, we derived Reaction (9).

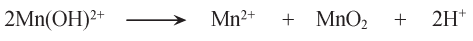

(9)

The resulting reaction equation is as follows (Reaction (10)), and the relationship between the amount of adsorption sites occupied by Pb^{2+} and the amount of Mn^{2+} released was $V_4 = 2M_4 = H_4$;

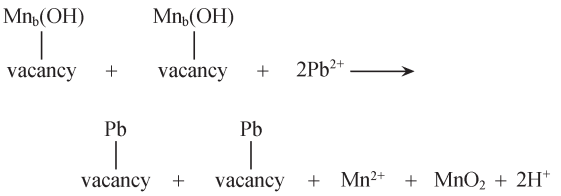

(10)

Consequently, the total side amount of vacant sites involved in the reactions was as Eq. (11).

$$V_{total} = H_1 + 1/2H_2 + M_3 + H_4 \quad (11)$$

Because $H_1 = P_1$, $H_4 = 2M_4$, then $H_1 = 1/2H_1 + 1/2P_1$, $H_4 = 1/2H_4 + M_4$, the total amount of adsorption sites, becomes as Eq. (12).

$$V_{total} = (1/2H_1 + 1/2P_1) + 1/2H_2 + M_3 + 1/2H_4 + M_4 = 1/2(H_1 + H_2 + H_4) + 1/2P_1 + (M_3 + M_4) = 1/2H_{total} + 1/2P_1 + M_{total} \quad (12)$$

where, H_{total} and M_{total} represent the total amount of H^+ and Mn^{2+} released during the adsorption process, respectively. V_{total} was also equal to the theoretic amount of Pb^{2+} adsorbed, which complied with the charge conservation law in the ion exchange reactions.

The ratio of the measured maximum amount of adsorbed Pb^{2+} to the corresponding total sides of vacant sites (A_{max}/V_{total}) was in the range of 0.94–1.25 (Table 4). For samples HB1, HB2, HB3, HB4, HB5, OHB1 and OHB2 with high Mn AOS, the ratio was in the range of 1.16–1.25, while for samples HB6, OHB3, OHB4, OHB6, OHB7, and OHB8 with low Mn AOS, the ratio was in the range of 0.94–1.08.

There was a highly significant linear correlation between A_{max}/V_{total} and the Mn AOS of the samples ($r = 0.8529 > 0.6614$, $n = 14$, α=0.01) (Fig. 5). When Mn AOS was low, the corresponding ratio was close to 1, implying that only one Pb^{2+} was adsorbed to one side of a vacant site. When the AOS of Mn was high, the corresponding ratio was slightly higher than 1, indicating that more than one Pb^{2+} were adsorbed on one side of a small part of vacant sites. In the case of two adsorbed Pb^{2+}, one was assumed to form a tridentate corner-sharing interlayer complex on the one side of a vacant site, and the other might form a triple

Table 4 Ratio of the measured maximum amount of adsorbed Pb^{2+} to the corresponding total sides of vacant sites (A_{max}/V_{total}) and Vtotal

H-birnessite	V_{total} (mmol/kg)	A_{max}/V_{total}	OH-birnessite	V_{total} (mmol/kg)	A_{max}/V_{total}
HB1	1982	1.24	OHB1	1581	1.15
HB2	1917	1.25	OHB2	1202	1.18
HB3	1811	1.20	OHB3	943	0.94
HB4	1663	1.25	OHB4	896	1.00
HB5	1534	1.25	OHB5	840	1.15
HB6	1223	1.08	OHB6	789	1.02
			OHB7	510	0.98
			OHB8	515	1.02

edge-sharing interlayer complex with neighboring layer MnO_6 octahedron on the one side of the empty tridentate cavity which is located near to the vacant site, such as the Pb coordination in quenselite (Manceau *et al*., 2002). When the amount of Pb^{2+} adsorbed was high, two Pb^{2+} adsorbed in the region of one side of a vacant site more likely occurred. Furthermore, high Mn AOS in samples made the great likelihood for two Pb^{2+} adsorbed in the region of one side of a vacant site, leading to a high ratio of maximum Pb^{2+} adsorption to the corresponding total of one side sites of vacant sites.

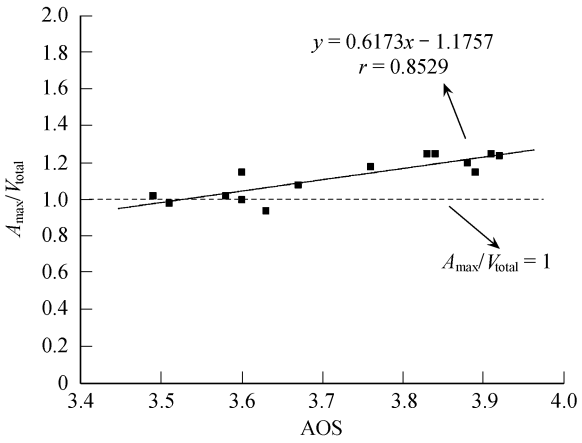

Fig. 5 Linear correlation between A_{max}/V_{total} and Mn AOS.

4 Conclusions

This study further confirmed that Pb^{2+} was likely adsorbed mainly above and below vacant sites in the structure of birnessite, and demonstrated that Mn^{2+}, H^+, and K^+ released during the adsorption were derived mostly from the corresponding cations adsorbed on the vacant sites. Additionally, when the amount of vacant cation sites increased, the maximum amount of adsorbed Pb^{2+} also increased, which led to the increase of the total amount of released Mn^{2+}, H^+, K^+, and the increased likelihood for two Pb^{2+} ions adsorbed in the region of one side of a vacant site. When the AOS of Mn in birnessite was high, almost no Mn^{2+} was released during the lead adsorption. Therefore, we can practise birnessite with high Mn AOS for utilization. In this case, it does not cause manganese pollution in the process of remediation of lead contaminated environments.

Acknowledgments

This work was financial supported by the National Natural Science Foundation of China (No. 40471070), the National Excellent Doctoral Dissertation of China (No. 200767). The authors gratefully acknowledge Ph.D. graduate student Matthew Siebecker, Dr. Caixian Tang and Prof. Huada Daniel Ruan for reviewing the final draft.

References

Anderson P R, Christensen T H, 1988. Distribution coefficients of cadmium cobalt, nickel, and zinc in soils. *European Journal of Soil Science*, 39: 15–22.

Appelo C A J, Postma D A, 1999. A consistent model for surface complexation on birnessite (-MnO_2) and its application to a column experiment. *Geochimica et Cosmochimica Acta*, 63 (19-20): 3039–3048.

Burns R G, 1976. The uptake of cobalt into ferromanganese nodules, soils, and synthetic manganese (IV) oxides. *Geochimica et Cosmochimica Acta*, 40 (1): 95–102.

Davis J A, Leckie J O, 1978. Surface ionization and complexation at the oxide/water interface: II. Surface properties of amorphous iron oxyhydroxide and adsorption of metal ions. *Journal of Colloid and Interface Science*, 67: 90–107.

Feng X H, Liu F, Tan W F, Liu X W, 2004. Synthesis of birnessite from the oxidation of Mn^{2+} by O_2 in alkali medium: effects of synthesis conditions. *Clays and Clay Minerals*, 52(2): 240–250.

Feng X H, Zhai L M, Tan W F, Liu F, He J Z, 2007. Adsorption and redox reactions of heavy metals on synthesized Mn oxide minerals. *Environmental Pollution*, 147(2): 366–373.

Gadde R R, Laitinen H A, 1974. Studies of heavy metal adsorption by hydrous iron and manganese oxides. *Analytical Chemistry*, 46: 2022–2026.

Gaillot A C, Flot D, Drits V A, Manceau A, 2003. Structure of synthetic K-rich birnessite obtained by high-temperature decomposition of $KMnO_4$. I. Two-layer polytype from 800°C experiment. *Chemistry of Materials*, 15(24): 4666–4678.

Giles C H, MacEwan T H, Nakhwa S N, Smith D, 1960. Studies in adsorption Part XI. A system of classification of solution adsorption isotherms and its use in diagnosis of adsorption mechanisms and in measurement of specific surface area of solids. *Journal of Chemical Society*, 3: 3973–3993.

Golden D C, Chen C C, Dixon J B, 1987. Transformation of birnessite to buserite, todorokite, and manganite under mild hydrothermal treatment. *Clays and Clay Minerals*, 35(4): 271–280.

Hohl H, Stumm W, 1976. Interaction of Pb^{2+} with hydrous γ-Al_2O_3. *Journal of Colloid and Interface Science*, 55: 281–288.

Kijima N, Yasuda H, Sato T, Yoshimura Y, 2001. Preparation and characterization of open tunnel oxide [alpha]-MnO_2 precipitated by ozone oxidation. *Journal of Solid State Chemistry*, 159(1): 94–102.

Kinniburgh D G, 1986. General purpose adsorption isotherms. *Environmetal Science and Technology*, 20: 895–904.

Lanson B, Drits V A, Feng Q, Manceau A, 2002a. Structure of synthetic Na-birnessite: Evidence for a triclinic one-layer unit cell. *American Mineralogist*, 87(11-12): 1662–1671.

Lanson B, Drits V A, Gaillot A C, Silvester E, Plancon A, Manceau A, 2002b. Structure of heavy-metal sorbed birnessite: Part 1. Results from X-ray diffraction. *American Mineralogist*, 87(11-12): 1631–1645.

Lanson B, Drits V A, Silvester E, Manceau A, 2000. Structure of H-exchanged hexagonal birnessite and its mechanism of formation from Na-rich monoclinic buserite at low pH. *American Mineralogist*, 85(5-6): 826–838.

Manceau A, Charlet L, 1992. X-ray absorption spectroscopic study of the sorption of Cr(III) at the oxide-water interface: I. Molecular mechanism of Cr(III) oxidation on Mn oxides. *Journal of Colloid and Interface Science*, 148(2): 425–442.

Manceau A, Lanson B, Drits V A, 2002. Structure of heavy metal sorbed birnessite. Part III: Results from powder and polarized extended X-ray absorption fine structure spectroscopy. *Geochimica et Cosmochimica Acta*, 66(15): 2639–2663.

Matocha C J, Elzinga E J, Sparks D L, 2001. Reactivity of Pb(II) at the Mn(III,IV) (oxyhydr) oxide-water interface. *Environmetal Science and Technology*, 35(14): 2967–2972.

McKenzie R M, 1971. The synthesis of birnessite, cryptomelane, and some other oxides and hydroxides of manganese. *Mineralogical Magazine*, 38: 493–502.

McKenzie R M, 1979. Proton release during adsorption of heavy metal ions by a hydrous manganese dioxide. *Geochimica et Cosmochimica Acta*, 43: 1855–1857.

McKenzie R M, 1980a. The adsorption of lead and other heavy metals on oxides of manganese and iron. *Australian Journal of Soil Research*, 18(1): 61–73.

Mckenzie R M, 1980b. The manganese oxides in soils. In: Varentsov I M, Grasselly G Eds., Geology and Geochemistry of manganese, Vol. 1. Budapest: Hungarian Academy of Science: 259–269.

Murray J W, 1975. The interaction of metal ions at the manganese dioxide-solution interface. *Geochimica et Cosmochimica Acta*, 39: 505–519.

O'Reilly S E, Hochella M F, 2003. Lead sorption efficiencies of natural and synthetic Mn and Fe-oxides. *Geochimica et Cosmochimica Acta*, 67(23): 4471–4487.

Peacock C L, Sherman D M, 2007. Sorption of Ni by birnessite: Equilibrium controls on Ni in seawater. *Chemical Geology*, 238(1-2): 94–106.

Post J E, 1999. Manganese oxide minerals: Crystal structures and economic and environmental significance. *Proceeding of the National Academy of Sciences of the United States of America*, 96(7): 3447–3454.

Spark K M, Johnson B B, Wells J D, 1995. Characterizing heavy-metal adsorption on oxides and oxyhydroxides. *European Journal of Soil Science*, 46: 621–631.

Tu S, Racz G J, Goh T B, 1994. Transformations of synthetic birnessite as affected by pH and manganese concentration. *Clays and Clay Minerals*, 42(3): 321–330.

Villalobos M, Lanson B, Manceau A, Toner B, Sposito G., 2006. Structural model for the biogenic Mn oxide produced by *Pseudomonas putida*. *American Mineralogist*, 91(4): 489–502.

Villalobos M, Toner B, Bargar J, Sposito G., 2003. Characterization of the manganese oxide produced by *Pseudomonas putida* strain MnB1. *Geochimica et Cosmochimica Acta*, 67(14): 2649–2662.

Webb S M, Tebo B M, Bargar J R, 2005. Structural characterization of biogenic Mn oxides produced in seawater by the marine *Bacillus* sp. strain SG-1. *American Mineralogist*, 90(8-9): 1342–1357.

Zhao W, Cui H J, Feng X H, Tan W F, Liu F, 2009. Relationship between Pb^{2+} adsorption and average Mn oxidation state in synthetic birnessites. *Clays and Clay Minerals* (in press).